P5.4 USING WSR-88D DATA TO ASSESS THE INTENSITY OF THE COUPLED TERM IN THE SPECTRUM WIDTH EQUATION

Ming Fang [1]*, Richard J. Doviak[2] and Bruce Albrecht[1]

1. *Rosenstiel School of Marine and Atmospheric Science, University of Miami, Miami, Florida*
2. *National Severe Storms Laboratory, Norman, Oklahoma*

1. Introduction

The often used spectrum width equation is (Doviak and Zrnić, 2006, Section 5.3)

$$\sigma_v^2 = \sigma_s^2 + \sigma_\alpha^2 + \sigma_d^2 + \sigma_o^2 + \sigma_t^2, \quad (1)$$

where, σ_s, σ_α, σ_d, σ_o, and σ_t, represent the spectrum widths due to mean wind shear, antenna rotation, dispersion of hydrometeor terminal velocities, hydrometer's oscillation and/or wobbling, and turbulence. Fang and Doviak (2008), through a rigorous derivation, showed (1) is valid only for the expected Doppler spectrum or the expected value of measured σ_v^2. Furthermore, the variance associated with shear and antenna rotation cannot be separated into a sum of second central moments as implied by (1). For a scanning beam directed at low elevation angles, the spectrum width equation they propose (Fang and Doviak , 2008, Eq. B13) is

$$\overline{\hat{\sigma}_v^2(\vec{r},t_n)}^{(e)} = \overline{\sigma_s^2(\vec{r})}^{(e)} + \sigma_\alpha^2 + \overline{\sigma_o^2(\vec{r})}^{(e)} + \overline{\hat{\sigma}_t^2(\vec{r},t_n)}^{(e)} + T_c^{(e)}, \quad (2a)$$

where

$$T_c^{(e)} = \overline{2\delta v_s(\vec{r})\delta\hat{v}_t(\vec{r},t_n)}^{(e)}. \quad (2b)$$

For the cases of stratiform weather presented herein, $\delta v_s(\vec{r})$ is principally a function of height and thus it can be shown that only vertical shear of large scale turbulence couples with mean wind shear to significantly contribute to $T_c^{(e)}$. At low elevation angles the σ_d^2 term can be ignored and thus it is not included in (2). Herein, the over bar emphasizes that the variable is a spatial average weighted by the antenna beam pattern and reflectivity field, $\vec{r}$ is the vector range over which spatial average is performed, the superscript (e) indicates that an effective beam pattern defines the scanning resolution volume $V_6^{(e)}$ (Doviak and Zrnic, 2006, Section 4.4.4), and the diacritical circumflex emphasizes that the marked variable is an estimate made from data collected over a short dwell time (typically a few tens of milliseconds) at t_n. To shorten notation, the argument $(\vec{r},t_n)$ henceforth will not be displayed. The most remarkable difference between (1) and (2) is that (2) has an extra term, the so-called coupled term $T_c^{(e)}$. Through this term, mean wind v_s and turbulence v_t are coupled together.

Using the published data given by Hocking (1988), Fang and Doviak (2008) calculated the standard deviation of the coupled term and concluded its magnitude was compatible with the standard deviation of σ_v^2 due to processing finite signal samples, and therefore it was significant. However, Hocking's data was obtained with long wavelength (i.e., λ = 1506 m) vertically pointed radar sampling clear air scattering from about 80 km above ground. Thus estimating the variance of $T_c^{(e)}$ and its significance for weather radar observations is the focus of this study.

* *Corresponding author address*: Ming Fang, 4600 Rickenbacker causeway, Miami, FL 33149; email: mfang@rsmas.miami.edu

Because $T_c^{(e)}$ is a zero mean random variable, its variance is the parameter that needs to be evaluated. Thus the following Section 2 develops an analytical equation which expresses the variances of terms in (2). Section 3 calculates various variances including the variance of coupled term using data collected with weather radar. Section 4 introduces another method to estimate the variance of coupled term and compares the results. A summary and conclusions are given in Section 5.

2. The equation relating variances of terms in the spectrum width equation

Because $\overline{\hat{\sigma}_o^2}^{(e)}$ is typically small (i.e., less than 0.1 m^2s^{-2}; Zrnic and Doviak, 1989) compared to other spectral broadening terms, it can be ignored and (2a) can be expressed as

$$\overline{\hat{\sigma}_v^2}^{(e)} - \overline{\hat{\sigma}_s^2}^{(e)} - \sigma_\alpha^2 = \overline{\hat{\sigma}_t^2}^{(e)} + T_c^{(e)}. \qquad (3a)$$

It is noteworthy that $\overline{\sigma_s^2}^{(e)}$ in (2) has been changed to $\overline{\hat{\sigma}_s^2}^{(e)}$. In the derivation leading to (2a) it has been assumed that mean wind is perfectly known. In analyzing weather data however, mean wind must be estimated from data; thus the mean estimates will have some uncertainty. Nevertheless, this uncertainty or variance is very small (Appendix A) for the stratiform weather cases to be presented herein. Because σ_α^2 is deterministic it does not have variance. Thus the variance of left side of (3a) is completely attributed to the fluctuation of $\overline{\hat{\sigma}_v^2}^{(e)}$, and its variance can thus be expressed as

$$\mathrm{Var}_v\left[\overline{\hat{\sigma}_v^2}^{(e)}\right] = \mathrm{Var}_v\left[\overline{\hat{\sigma}_t^2}^{(e)}\right] + \mathrm{Var}_v\left[T_c^{(e)}\right] + \mathrm{Cov}_v\left[\overline{\hat{\sigma}_t^2}^{(e)} T_c^{(e)}\right]. \qquad (3b)$$

In the derivation of (2) the ensemble average over the scatterers' configurations and backscattering cross sections had been made (Fang and Doviak, 2008; the subscript 'v' denotes variance associated with changes in the velocity field). But $\overline{\hat{\sigma}_v^2}^{(e)}$ estimates are made with weather radar using data taken over short dwell times, and those ensemble averages are therefore not made. Thus the observed variance, $\mathrm{Var}_{obs}\left[\overline{\hat{\sigma}_v^2}^{(e)}\right]$, is associated both with the changes of the scatterers' configuration, as well as changes of the velocity field. That is

$$\mathrm{Var}_{obs}\left[\overline{\hat{\sigma}_v^2}^{(e)}\right] = \mathrm{Var}_v\left[\overline{\hat{\sigma}_v^2}^{(e)}\right] + \mathrm{Var}_{sc}\left[\overline{\hat{\sigma}_v^2}^{(e)}\right] \qquad (4a)$$

where $\mathrm{Var}_{sc}\left[\overline{\hat{\sigma}_v^2}^{(e)}\right]$ is the variance due to changes in the scatterers' configurations, (this is the variance addressed by most radar meteorologists when computing errors in estimating $\overline{\hat{\sigma}_v^2}^{(e)}$), whereas $\mathrm{Var}_v\left[\overline{\hat{\sigma}_v^2}^{(e)}\right]$ is principally due to the change of large scale turbulence across the resolution volume. Mean Doppler velocity as well as the width of the spectrum change from estimate to estimate, but the focus of this study is on the fluctuations in the second central moment of the estimated Doppler spectra. Substituting (3a) into (4a), the following result is obtained:

$$\mathrm{Var}_{obs}\left[\overline{\hat{\sigma}_v^2}^{(e)}\right] = \mathrm{Var}_v\left[\overline{\hat{\sigma}_t^2}^{(e)}\right] + \mathrm{Var}_v\left[T_c^{(e)}\right] + \mathrm{Cov}_v\left[\overline{\hat{\sigma}_t^2}^{(e)} T_c^{(e)}\right] + \mathrm{Var}_{sc}\left[\overline{\hat{\sigma}_v^2}^{(e)}\right], \qquad (4b)$$

2.1 *The covariance of spectrum width due to turbulence and the coupled term*

Arguments are in this section presented to show $\mathrm{Cov}_v\left[\overline{\hat{\sigma}_t^2}^{(e)} T_c^{(e)}\right]$ is negligibly small. To simplify

the analysis without losing its objective, let's assume the radar beam is fixed so that $\mathrm{Cov}_\mathrm{v}\left[\overline{\hat{\sigma}_\mathrm{t}^2}^{(\mathrm{e})} T_\mathrm{c}^{(\mathrm{e})}\right]$ can be expressed as $\mathrm{Cov}_\mathrm{v}\left[\overline{\hat{\sigma}_\mathrm{t}^2} T_\mathrm{c}\right]$. If the vertical spectrum $S(K_\mathrm{z})$ of horizontal wind has a K_z^{-3} power law dependence on wavenumber as the few meager measurements suggest for quiescent weather conditions (i.e., Endlich et al., 1969), theory (Doviak, et al., 2008) shows the spectral coefficients contributing most significantly to T_c are those from around the peak of $S(K_\mathrm{z})$. In this case turbulence at scales about 5 km contributes most to T_c, whereas the turbulent eddy of scale Λ_e = 0.3 km contributes most to $\overline{\hat{\sigma}_\mathrm{t}^2}$ (Fang 2008, Section 10). The correlation between $\overline{\hat{\sigma}_\mathrm{t}^2}$ and T_c depends on the wavenumber separation between the spectral coefficients that contribute to each. If the separation is large, the coefficients are statistically independent (Batchelor, 1960, p. 112). Because the eddies that significantly contribute to T_c are far removed from those that contribute to $\overline{\hat{\sigma}_\mathrm{t}^2}$, we conclude $\overline{\hat{\sigma}_\mathrm{t}^2}$ and T_c are not strongly correlated; thus $\mathrm{Cov}_\mathrm{v}\left[\overline{\hat{\sigma}_\mathrm{t}^2} T_\mathrm{c}\right] \approx 0$

A physical argument that supports the above conclusion is now presented for stratiform weather cases examined herein. Consider that in absence of strong convection there is little coupling between flows at various levels. Thus vertical perturbations in the horizontal flow would be generated as regions of higher (lower) horizontal momentum are differentially transported, by a vertically sheared mean wind, to be above regions of lower (higher) momentum. These vertical perturbations of the horizontal flow likely formed the spectrum $S(K_\mathrm{z})$ reported by Endlich et al, (1969). Such transport likely also occurs in stratiform precipitation in which vertical shear is strong and convection is weak. Furthermore, long horizontal scales (i.e., tens and hundreds of kilometers) have relatively large spectral intensity (Vinnichenko and Dutton, 1969, Nastrom and Gage, 1985). Thus equally large spectral intensity (i.e., velocity variance) would exist at smaller vertical scales. Doviak et al., (2008) show turbulence at vertical scales larger than $\mathrm{V}_6^{(\mathrm{e})}$ contributes most significantly to T_c. Thus, based on this argument one should expect the larger and more energetic vertical scales of the differentially advected horizontal velocity perturbations mostly contribute to T_c, and these are uncorrelated with the smaller scales of turbulence, often generated in situ, that principally contribute to $\overline{\hat{\sigma}_\mathrm{t}^2}$. In conclusion it appears reasonable to accept the hypothesis that $\mathrm{Cov}\left[\overline{\hat{\sigma}_\mathrm{t}^2}^{(\mathrm{e})} T_\mathrm{c}^{(\mathrm{e})}\right] \approx 0$, and (4b) then simplifies to

$$\mathrm{Var}_{\mathrm{obs}}\left[\overline{\hat{\sigma}_\mathrm{v}^2}^{(\mathrm{e})}\right] = \mathrm{Var}\left[\overline{\hat{\sigma}_\mathrm{t}^2}^{(\mathrm{e})}\right] + \mathrm{Var}\left[T_\mathrm{c}^{(\mathrm{e})}\right] + \mathrm{Var}_{\mathrm{sc}}\left[\overline{\hat{\sigma}_\mathrm{v}^2}^{(\mathrm{e})}\right] \quad (5)$$

2.2 *The variance equation with quantization*

Because spectrum width data recorded by WSR-88D radar is coarsely quantized (Fig. 1), the variance associated with quantization needs to be considered. Appendix B shows quantization variance $\mathrm{Var}_\mathrm{q}\left[\sqrt{\overline{\hat{\sigma}_\mathrm{v}^2}^{(\mathrm{e})}}\right]$ is significant and should be included in the variance equation. Thus (5) is then expressed as

$$\mathrm{Var}_{\mathrm{obs}}\left[\overline{\hat{\sigma}_\mathrm{v}^2}^{(\mathrm{e})}\right] + \mathrm{Var}_\mathrm{q}\left[\overline{\hat{\sigma}_\mathrm{v}^2}^{(\mathrm{e})}\right] = \mathrm{Var}_\mathrm{v}\left[\overline{\hat{\sigma}_\mathrm{t}^2}^{(\mathrm{e})}\right] + \mathrm{Var}_\mathrm{v}\left[T_\mathrm{c}^{(\mathrm{e})}\right] + \mathrm{Var}_{\mathrm{sc}}\left[\overline{\hat{\sigma}_\mathrm{v}^2}^{(\mathrm{e})}\right] \quad (6)$$

This equation will be the focus of attention. To deduce $\mathrm{Var}_\mathrm{v}\left[T_\mathrm{c}^{(\mathrm{e})}\right]$ the variances for terms on the both sides of the above equation will be calculated.

3. Calculating the various variances

In the following subsections variances of the terms in (6) are calculated. We consider stratiform weather for which the horizontal turbulence contributing significantly to $\overline{\hat{\sigma}_\mathrm{t}^2(\vec{r},t_n)}$ is 2D horizontally isotropic and homogeneous. Because weather radar observations are typically made at low elevation angles, the radial component of wind observed by Doppler radar is principally due to the horizontal wind components. Thus it is reasonable to focus attention on the spectral characteristics of the horizontal component of turbulence. The assumption of 2-D isotropy is supported by observations of Vinnichenko and Dutton (1969) and Nastrom and Gage (1985). These observations show spatial spectra of horizontal turbulence to be 2D horizontally isotropic for wavelengths from the order of tens of kilometers to least 2 km. Most of these data were collected by aircraft and balloon soundings, and apply principally to fair weather turbulence. But we assume these results are also applicable to the stratiform weather where the convection is weak.

3.1 *The variance of the spectrum width associated with turbulence*

It can be shown (Fang, 2008, Section 10) were

$$\mathrm{Var}_\mathrm{v}\left[\overline{\hat{\sigma}_\mathrm{t}^2}^{(\mathrm{e})}\right]=c_1\mathrm{E}_\mathrm{v}^2\left[\overline{\hat{\sigma}_\mathrm{t}^2}^{(\mathrm{e})}\right], \qquad (7)$$

c_1, the factor of proportionality, is ≤ 1. Equation (7) is the basis for us to calculate $\mathrm{Var}_\mathrm{v}\left[\overline{\hat{\sigma}_\mathrm{t}^2}^{(\mathrm{e})}\right]$ from radar measured data. Taking the expectation of (3a) over the ensemble of velocity fields, noting $E_\mathrm{v}\left[T_\mathrm{c}^{(\mathrm{e})}\right]=0$, gives

$$\mathrm{E}_\mathrm{v}\left[\overline{\hat{\sigma}_\mathrm{t}^2}^{(\mathrm{e})}\right]=\mathrm{E}_\mathrm{v}\left[\overline{\hat{\sigma}_\mathrm{v}^2}^{(\mathrm{e})}-\overline{\hat{\sigma}_\mathrm{s}^2}^{(\mathrm{e})}-\sigma_\alpha^2\right]. \qquad (8)$$

The term on the right hand side of (8) can be calculated from observed radar data. If $\overline{\hat{\sigma}_\mathrm{t}^2}^{(\mathrm{e})}$ is statistically homogeneous and 2D horizontally isotropic, we can estimate $\mathrm{E}_\mathrm{v}\left[\overline{\hat{\sigma}_\mathrm{t}^2}^{(\mathrm{e})}\right]$ using the spatial average $\left\langle\left[\overline{\hat{\sigma}_\mathrm{v}^2}^{(\mathrm{e})}-\overline{\hat{\sigma}_\mathrm{s}^2}^{(\mathrm{e})}-\sigma_\alpha^2\right]\right\rangle_\mathrm{s}$, but the spatial average domain needs to be large enough, otherwise $\left\langle T_\mathrm{c}^{(\mathrm{e})}\right\rangle_s$ might not average to zero or to a sufficient small value so as not to bias the estimate of $\mathrm{E}_\mathrm{v}\left[\overline{\hat{\sigma}_\mathrm{t}^2\left(\vec{r},t_\mathrm{n}\right)}^{(\mathrm{e})}\right]$.

Fig. 1 shows the azimuth dependence of $\overline{\hat{\sigma}_\mathrm{v}^2}^{(\mathrm{e})}-\overline{\hat{\sigma}_\mathrm{s}^2}^{(\mathrm{e})}-\sigma_\alpha^2$ (equivalently $\overline{\hat{\sigma}_\mathrm{t}^2}^{(\mathrm{e})}+T_\mathrm{c}^{(\mathrm{e})}$) for two snow storms observed by the KLSX. Each $\overline{\hat{\sigma}_\mathrm{v}^2}^{(\mathrm{e})}-\overline{\hat{\sigma}_\mathrm{s}^2}^{(\mathrm{e})}-\sigma_\alpha^2$ datum in Fig. 1 is calculated using (3a) where $\overline{\hat{\sigma}_\mathrm{s}^2}^{(\mathrm{e})}$ is determined from a VAD analysis of the radial velocity data (Appendix A), and the second central moment $\sigma_\alpha^2 = 0.34\,\mathrm{m^2s^{-2}}$ is calculated using the parameters for the KSLX and the formulas presented by Doviak and Zrnic (2006, Section 5.3).

The pair of narrow peaks at 110° and 290° in Figs. 1a and 1b could be an artifact due to radiation from other radar because the peaks exist for both cases and remain in at fixed directions for data collected a year apart. If $T_\mathrm{c}^{(\mathrm{e})}$ were zero, Fig. 1 would be a plot of $\overline{\hat{\sigma}_\mathrm{t}^2}^{(\mathrm{e})}$.

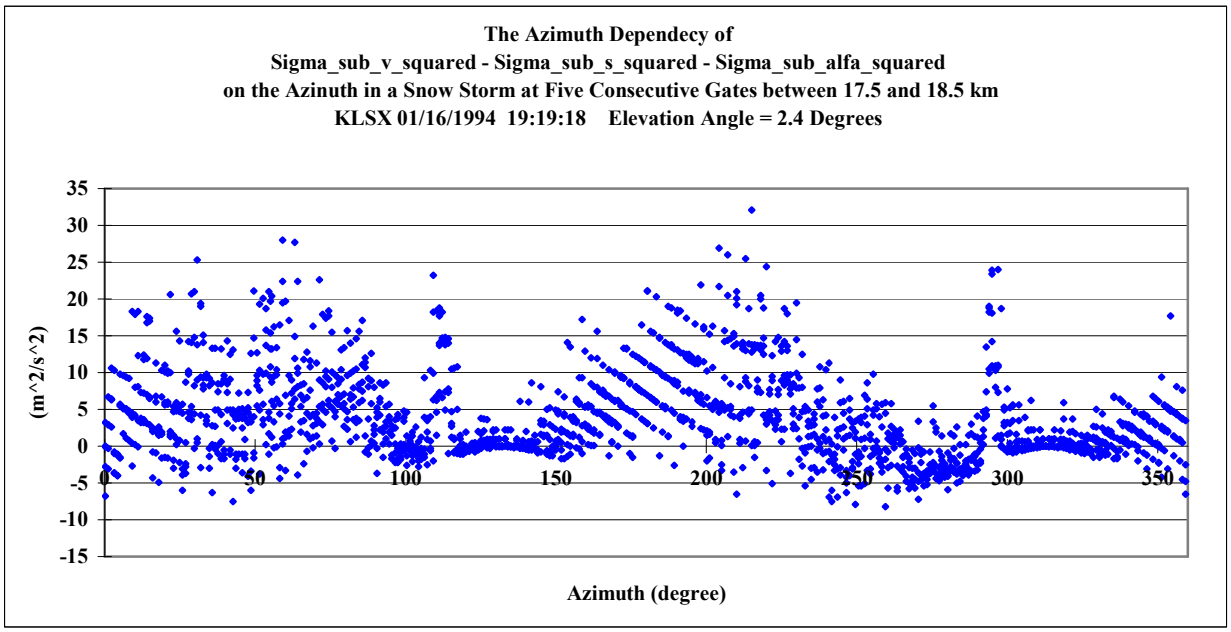

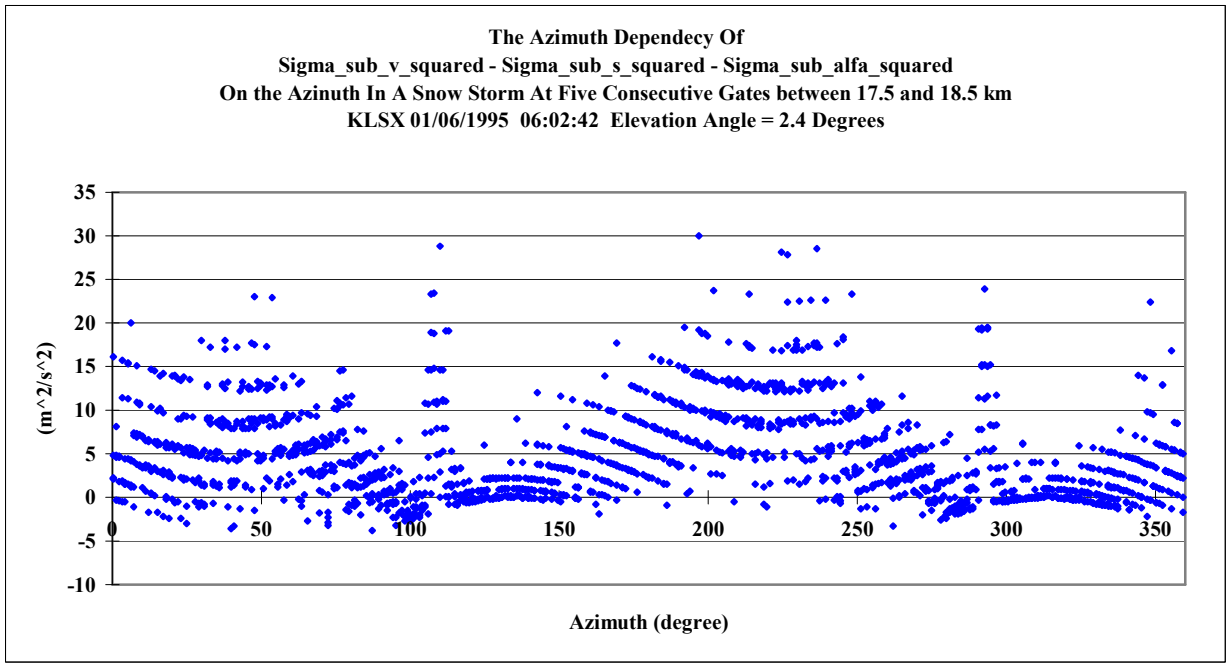

Fig. 1. Azimuth dependence of $\overline{\hat{\sigma}_{\mathrm{v}}^2\left(\vec{r},t_n\right)}^{(\mathrm{e})} - \overline{\hat{\sigma}_{\mathrm{s}}^2\left(\vec{r}\right)}^{(\mathrm{e})} - \sigma_{\alpha}^2$ for 2 snow storms observed by KTSX

Because $\overline{\hat{\sigma}_{\mathrm{t}}^2}^{(\mathrm{e})}$ is the second central moment of turbulence it cannot be negative. But if $\overline{\hat{\sigma}_{\mathrm{s}}^2}^{(\mathrm{e})}$ and/or σ_{α}^2 are overestimated, or $\overline{\hat{\sigma}_{\mathrm{v}}^2}^{(\mathrm{e})}$ is underestimated, $\overline{\hat{\sigma}_{\mathrm{t}}^2}^{(\mathrm{e})} + T_{\mathrm{c}}^{(\mathrm{e})}$ can be negative even if $T_{\mathrm{c}}^{(\mathrm{e})}$ is zero. It is common practice to attribute negative values of $\overline{\hat{\sigma}_{\mathrm{t}}^2}^{(\mathrm{e})}$ to these over and/or underestimates. Because the variance associated with the estimation of $\overline{\hat{\sigma}_{\mathrm{s}}^2\left(\vec{r}\right)}$ is

very small (Appendix A) $\overline{\hat{\sigma}_s^2}^{(e)}$ is unlikely to be overestimated. Furthermore σ_α^2 can be accurately calculated. Thus, negative values in the figures are primarily attributed to $T_c^{(e)}$.

The data shown in the Fig. 1 is obtained from five consecutive range locations of $V_6^{(2)}$ spaced 250 m. Only five range gates are used because of the need to limit the change of beam height to 52 m (at the 2.4° elevation angle) so that vertical variations of turbulence can be neglected. At the range of 20 km, beam width $\sigma_\theta r_0$ is about 100m. The arithmetic average of data in Fig.1 over 360° of azimuth is 3.8 m^2s^{-2}. Because $T_c^{(e)}$ is a zero mean random variable, this average should reduce $T_c^{(e)}$ to zero if the averaging domain contains a sufficient number of independent samples of $T_c^{(e)}$. If this were the case, the average would then be an estimate of $\overline{\hat{\sigma}_t^2}^{(e)}$. But the 3.8 m^2s^{-2} average is much larger than the spatial average of data around 130° and 310° where $\overline{\hat{\sigma}_s^2}^{(e)} \approx 0$ (Fang, 2008, section 9.3) and therefore $T_c^{(e)}$ should also equal zero. Either the average cannot effectively reduce $T_c^{(e)}$, or $\overline{\hat{\sigma}_t^2}^{(e)}$ is not horizontally homogeneous, or both. The fact that $T_c^{(e)}$ is mostly positive suggests that δv_s and δv_t are positively correlated. Large velocity perturbations in the direction of faster flow and weaker perturbation in slower flow is expected, and thus it is natural δv_s and δv_t are positively correlated.

Because $T_c^{(e)}$ is zero around 130° and 310°, the spatial average $\left\langle \left[\overline{\hat{\sigma}_v^2}^{(e)} - \overline{\hat{\sigma}_s^2}^{(e)} - \sigma_\alpha^2 \right] \right\rangle_s$ equals $\left\langle \overline{\hat{\sigma}_t^2}^{(e)} \right\rangle_s$. Thus using data at five consecutive range gates that lie in 3° sectors centered at these two directions,

$$E_v\left[\overline{\hat{\sigma}_t^2}^{(e)}\right] \approx \left\langle \overline{\hat{\sigma}_t^2}^{(e)} \right\rangle_s = \frac{1}{30}\sum_{i=1}^{30}\left[\overline{\hat{\sigma}_t^2}^{(e)}\right]_i = 0.57 m^2 s^{-2}. \quad (9)$$

By taking c_1 = 1 in (7), the variance of $\overline{\hat{\sigma}_t^2(\vec{r},t_n)}^{(e)}$ is at most

$$\mathrm{Var}_v\left[\overline{\hat{\sigma}_t^2}^{(e)}\right] = \mathrm{E}_v^2\left[\overline{\hat{\sigma}_t^2}^{(e)}\right] = \left(0.57 m^2 s^{-2}\right)^2 = 0.32 m^4 s^{-4}. \quad (10)$$

for the data presented in Fig. 1a. For the case presented in Fig. 1b,

$$\mathrm{E}_v\left[\overline{\hat{\sigma}_t^2}^{(e)}\right] = \left\langle \overline{\hat{\sigma}_t^2}^{(e)} \right\rangle_s = 1.2 m^2 s^{-2}, \quad (11a)$$

and for this case,

$$\mathrm{Var}_v\left[\overline{\hat{\sigma}_t^2}^{(e)}\right] = \mathrm{E}_v^2\left[\overline{\hat{\sigma}_t^2}^{(e)}\right] = \left(1.2 m^2 s^{-2}\right)^2 = 1.44 m^4 s^{-4}. \quad (11b)$$

Because the variance of $\overline{\hat{\sigma}_s^2}^{(e)}$ is very small, the negative values in Fig 1 are attributed to $T_c^{(e)}$.

3.2 *The variance of the observed spectrum width squared*

Because variances of $\overline{\hat{\sigma}_s^2}^{(e)}$ and σ_α^2 are negligible, it is deduced from (3a) that $\mathrm{Var}_{obs}\left[\overline{\hat{\sigma}_v^2}^{(e)}\right]$ = $\mathrm{Var}_{obs}\left[\overline{\hat{\sigma}_v^2}^{(e)} - \overline{\hat{\sigma}_s^2}^{(e)} - \sigma_\alpha^2\right]$ and is computed vs azimuth using the following formula,

$$\mathrm{Var}_{\mathrm{obs}}\left[\overline{\hat{\sigma}_{\mathrm{v}}^{2}}^{(\mathrm{e})}\right]=\mathrm{E}_{\mathrm{v,sc}}\left[\left\{\left(\overline{\hat{\sigma}_{\mathrm{v}}^{2}}^{(\mathrm{e})}-\overline{\hat{\sigma}_{\mathrm{s}}^{2}}^{(\mathrm{e})}-\sigma_{\alpha}^{2}\right)-\mathrm{E}_{\mathrm{v,sc}}\left[\overline{\hat{\sigma}_{\mathrm{v}}^{2}}^{(\mathrm{e})}-\overline{\hat{\sigma}_{\mathrm{s}}^{2}}^{(\mathrm{e})}-\sigma_{\alpha}^{2}\right]\right\}^{2}\right]. \quad (12)$$

where subscript 'v and ,sc' is appended to the expectation operator E to emphasize the average is to been taken over the ensembles of both the velocity field and the scatterers' configurations.

The second term in the brackets on the right side of (12) is evaluated using the following procedure. The only term in (3a) that depends on the changes in the scatterers' configuration is $\overline{\hat{\sigma}_{\mathrm{v}}^{2}}^{(\mathrm{e})}$. Thus the ensemble average of (3a) can be expressed as

$$\mathrm{E}_{\mathrm{v,sc}}\left[\overline{\hat{\sigma}_{\mathrm{v}}^{2}}^{(\mathrm{e})}-\overline{\hat{\sigma}_{\mathrm{s}}^{2}}^{(\mathrm{e})}-\sigma_{\alpha}^{2}\right]=\mathrm{E}_{\mathrm{v}}\left[\overline{\hat{\sigma}_{\mathrm{t}}^{2}}^{(\mathrm{e})}+T_{\mathrm{c}}^{(\mathrm{e})}\right]. \quad (13)$$

Because $\mathrm{E}_{\mathrm{v}}\left[T_{\mathrm{c}}^{(\mathrm{e})}\right]$ = 0, (13) simplifies to

$$\mathrm{E}_{\mathrm{v,sc}}\left[\overline{\hat{\sigma}_{\mathrm{v}}^{2}}^{(\mathrm{e})}-\overline{\hat{\sigma}_{\mathrm{s}}^{2}}^{(\mathrm{e})}-\sigma_{\alpha}^{2}\right]=\mathrm{E}_{\mathrm{v}}\left[\overline{\hat{\sigma}_{\mathrm{t}}^{2}}^{(\mathrm{e})}\right], \quad (14)$$

substitution of (14) into (12) gives

$$\mathrm{Var}_{\mathrm{obs}}\left[\overline{\hat{\sigma}_{\mathrm{v}}^{2}}^{(\mathrm{e})}\right]=\mathrm{E}_{\mathrm{v,sc}}\left[\left\{\left(\overline{\hat{\sigma}_{\mathrm{v}}^{2}}^{(\mathrm{e})}-\overline{\hat{\sigma}_{\mathrm{s}}^{2}}^{(\mathrm{e})}-\sigma_{\alpha}^{2}\right)-\mathrm{E}_{\mathrm{v}}\left[\overline{\hat{\sigma}_{\mathrm{t}}^{2}}^{(\mathrm{e})}\right]\right\}^{2}\right] \quad (15)$$

As in Section 3a $\mathrm{E}_{\mathrm{v,sc}}\left[\overline{\hat{\sigma}_{\mathrm{v}}^{2}}^{(\mathrm{e})}-\overline{\hat{\sigma}_{\mathrm{s}}^{2}}^{(\mathrm{e})}-\sigma_{\alpha}^{2}\right]$ is estimated by spatially averaging over large horizontal domains.

Fig. 2 shows the plot of $\mathrm{Var}_{\mathrm{obs}}\left[\overline{\hat{\sigma}_{\mathrm{v}}^{2}}^{(\mathrm{e})}\right]$ calculated from data collected for the two snow storms observed by KLSX. The plot shows azimuth dependence of $\mathrm{Var}_{\mathrm{obs}}\left[\overline{\hat{\sigma}_{\mathrm{v}}^{2}}^{(\mathrm{e})}\right]$. Each point in the plot is calculated from data in a patch containing 10 radials and 5 range gates centered at 18 km. Thus the plot is a running average of data from 50 $\mathrm{V}_{6}^{(\mathrm{e})}$.

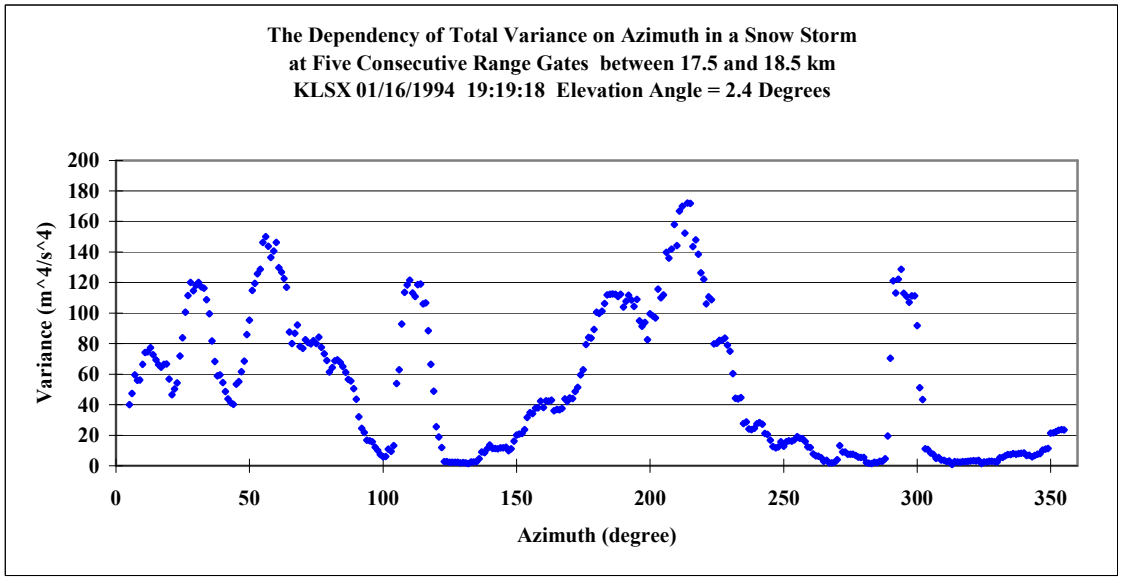

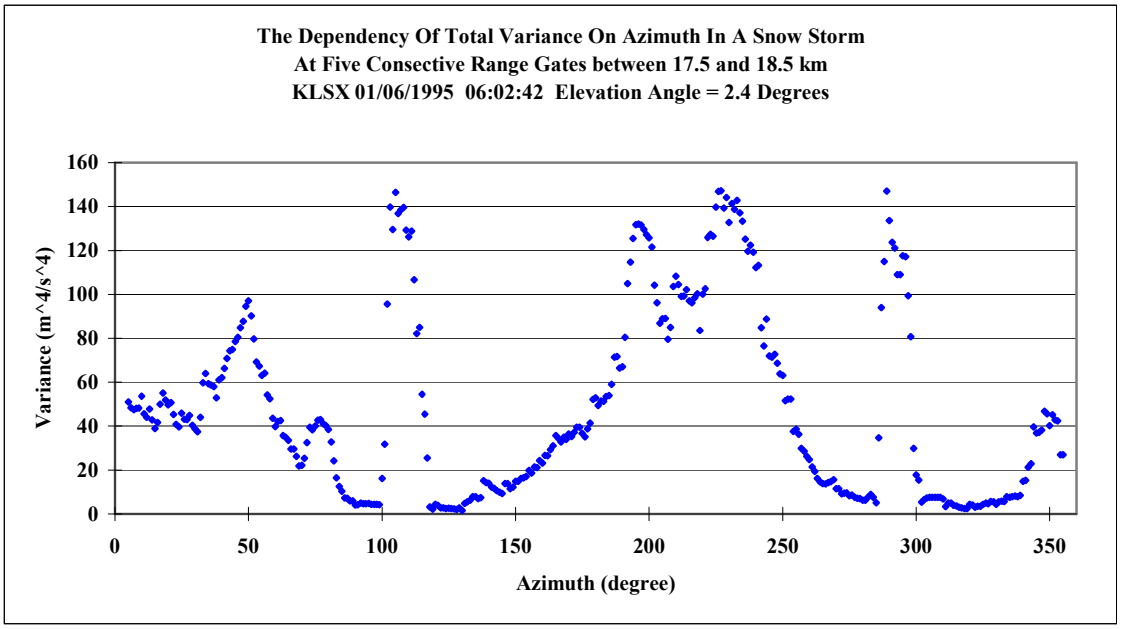

Fig. 2. Azimuth dependence of variance $\mathrm{Var}_{\mathrm{obs}}\left[\overline{\hat{\sigma}_{\mathrm{v}}^{2}}^{(\mathrm{e})}\right]$ of the observed spectrum width squared vs azimuth based on data collected with KLSX as in Fig.1.

3.3 *The variance associated with changes in scatterers' configuration*

Doviak and Zrnić (2006, section 6.5) discuss the variance due to changes in the scatterers' configuration (i.e., weather signal fluctuations). They present equations to compute $\mathrm{Var}_{\mathrm{sc}}\left[\sqrt{\overline{\hat{\sigma}_{\mathrm{v}}^{2}}^{(\mathrm{e})}}\right]$ ($\mathrm{Var}\left[\hat{\sigma}_{\mathrm{v}}\right]$ in their notation). For large signal to noise ratios, as has the data used herein, the equation to compute this variance is

$$\mathrm{Var}_{\mathrm{sc}}\left[\sqrt{\overline{\hat{\sigma}_{\mathrm{v}}^{2}}^{(\mathrm{e})}}\right]=\frac{3\lambda^{2}\sigma_{\mathrm{vn}}}{128\sqrt{\pi}MT_{\mathrm{s}}^{2}} \tag{16}$$

where λ is the radar wavelength (i.e., ≈ 0.1 m); M (≈ 50) is the number of samples, T_{s} (≈ 1 ms) is the pulse repetition time, and σ_{vn} is the normalized spectrum width defined as

$$\sigma_{\mathrm{vn}}=\frac{\sqrt{\overline{\sigma_{\mathrm{v}}^{2}}^{(\mathrm{e})}}}{2v_{\mathrm{a}}}=\frac{2T_{\mathrm{s}}\sqrt{\overline{\sigma_{\mathrm{v}}^{2}}^{(\mathrm{e})}}}{\lambda} \tag{17}$$

where $v_{\mathrm{a}}=\lambda/4T_{\mathrm{s}}$ is the unambiguous velocity, and $\overline{\sigma_{\mathrm{v}}^{2}}^{(\mathrm{e})}$ is the expected second central moment.

We need variance of $\overline{\hat{\sigma}_{\mathrm{v}}^{2}}$ whereas (17) gives the variance of $\sqrt{\overline{\hat{\sigma}_{\mathrm{v}}^{2}}}$. But $\mathrm{Var}_{\mathrm{sc}}\left[\overline{\hat{\sigma}_{\mathrm{v}}^{2}}^{(\mathrm{e})}\right]$ can be related to $\mathrm{Var}_{\mathrm{sc}}\left[\sqrt{\overline{\hat{\sigma}_{\mathrm{v}}^{2}}^{(\mathrm{e})}}\right]$ by the approximate formula (Papoulis, 2003, p.150)

$$\mathrm{Var}_{\mathrm{sc}}\left[\overline{\hat{\sigma}_{\mathrm{v}}^{2}}^{(\mathrm{e})}\right]=4\mathrm{E}_{\mathrm{v}}^{2}\left[\sqrt{\overline{\hat{\sigma}_{\mathrm{v}}^{2}}^{(\mathrm{e})}}\right]\mathrm{Var}_{\mathrm{sc}}\left[\sqrt{\overline{\hat{\sigma}_{\mathrm{v}}^{2}}^{(\mathrm{e})}}\right]. \tag{18}$$

By substituting (16) and (17) into (18), and using spectrum width data, we can compute the variance due to weather signal fluctuations caused by changes in the scatterers' configuration. Fig. 3 shows the azimuth

dependence of the variance (i.e. $\mathrm{Var}_{sc}\left[\overline{\hat{\sigma}_v^2}^{(e)}\right]$) for a snow storm observed with KLSX. The variance plot for the second snow storm corresponding to Fig. 1b is quite similar to that shown in Fig. 3. Each point in the plot corresponds to a value of $\mathrm{Var}_{sc}\left[\overline{\hat{\sigma}_v^2}^{(e)}\right]$ computed from (18). $\mathrm{E}_v^2\left[\sqrt{\overline{\hat{\sigma}_v^2}^{(e)}}\right]$ is calculated by squaring the running average of observed spectrum width at 10 radials and 5 consecutive range gates. Because $\mathrm{Var}_{sc}\left[\overline{\hat{\sigma}_v^2}^{(e)}\right]$ is proportional to $\mathrm{E}_v^2\left[\sqrt{\overline{\hat{\sigma}_v^2}^{(e)}}\right]$ as shown by (18), and because $\overline{\hat{\sigma}_v^2}^{(e)}$ is strongly dependent on $\overline{\hat{\sigma}_s^2}^{(e)}$ (Fig. A2), the two broad peaks in Fig. 3 are correlated with $\overline{\hat{\sigma}_s^2}^{(e)}$

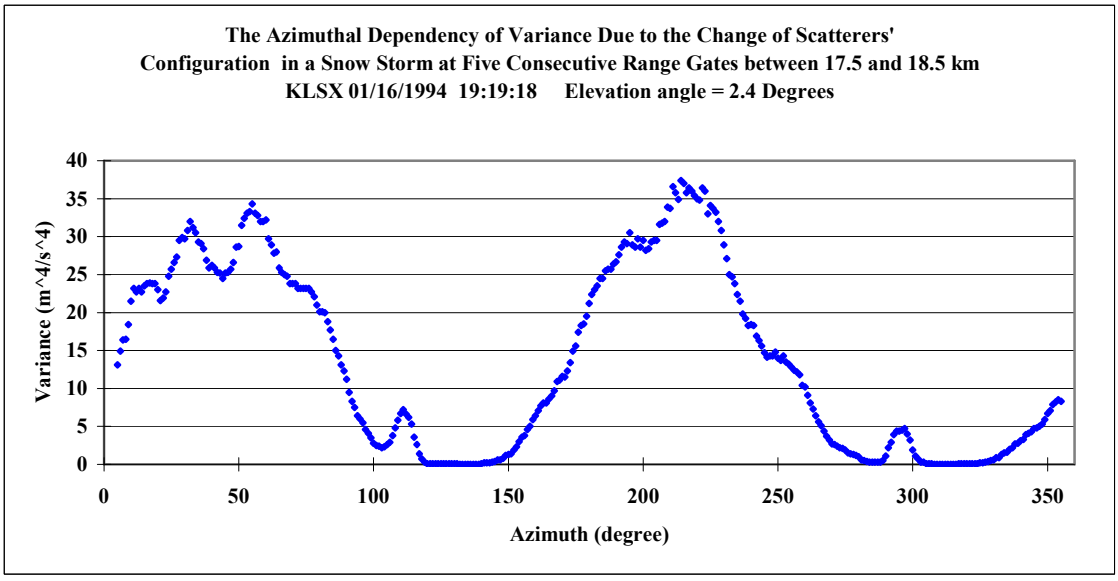

Fig. 3 Azimuth dependence of variance $\mathrm{Var}_{sc}\left[\overline{\hat{\sigma}_v^2}^{(e)}\right]$ due to weather signal fluctuations caused by changes in scatterers' configuration for the same data set shown in Fig. 1a.

3.4 *The variance of the coupled term*

It finally comes to the point to calculate $\mathrm{Var}_v\left[T_c^{(e)}\right]$ using (6) expressed as

$$\mathrm{Var}_v\left[T_c^{(e)}\right] = \mathrm{Var}_{obs}\left[\overline{\hat{\sigma}_v^2}^{(e)}\right] + \mathrm{Var}_q\left[\overline{\hat{\sigma}_v^2}^{(e)}\right] - \mathrm{Var}_v\left[\overline{\hat{\sigma}_t^2}^{(e)}\right] - \mathrm{Var}_{sc}\left[\overline{\hat{\sigma}_v^2}^{(e)}\right]. \quad (19)$$

The plots in Fig. 4 show the azimuth dependence of $\mathrm{Var}_v\left[T_c^{(e)}\right]$, as well as the variances $\mathrm{Var}_{sc}\left[\overline{\hat{\sigma}_v^2}^{(e)}\right]$ and $\mathrm{Var}_{obs}\left[\overline{\hat{\sigma}_v^2}^{(e)}\right]$ for comparison; the other variance terms are much smaller. There are a few negative value s in Fig. 4. Variance is a squared variable, it should nev er be negative. But because $\mathrm{Var}_v\left[T_c^{(e)}\right]$ is calculated f rom the sum and differences of other variances that are estimates, $\mathrm{Var}_v\left[T_c^{(e)}\right]$ fluctuates around about its true positive value and thus it likely creates some negative

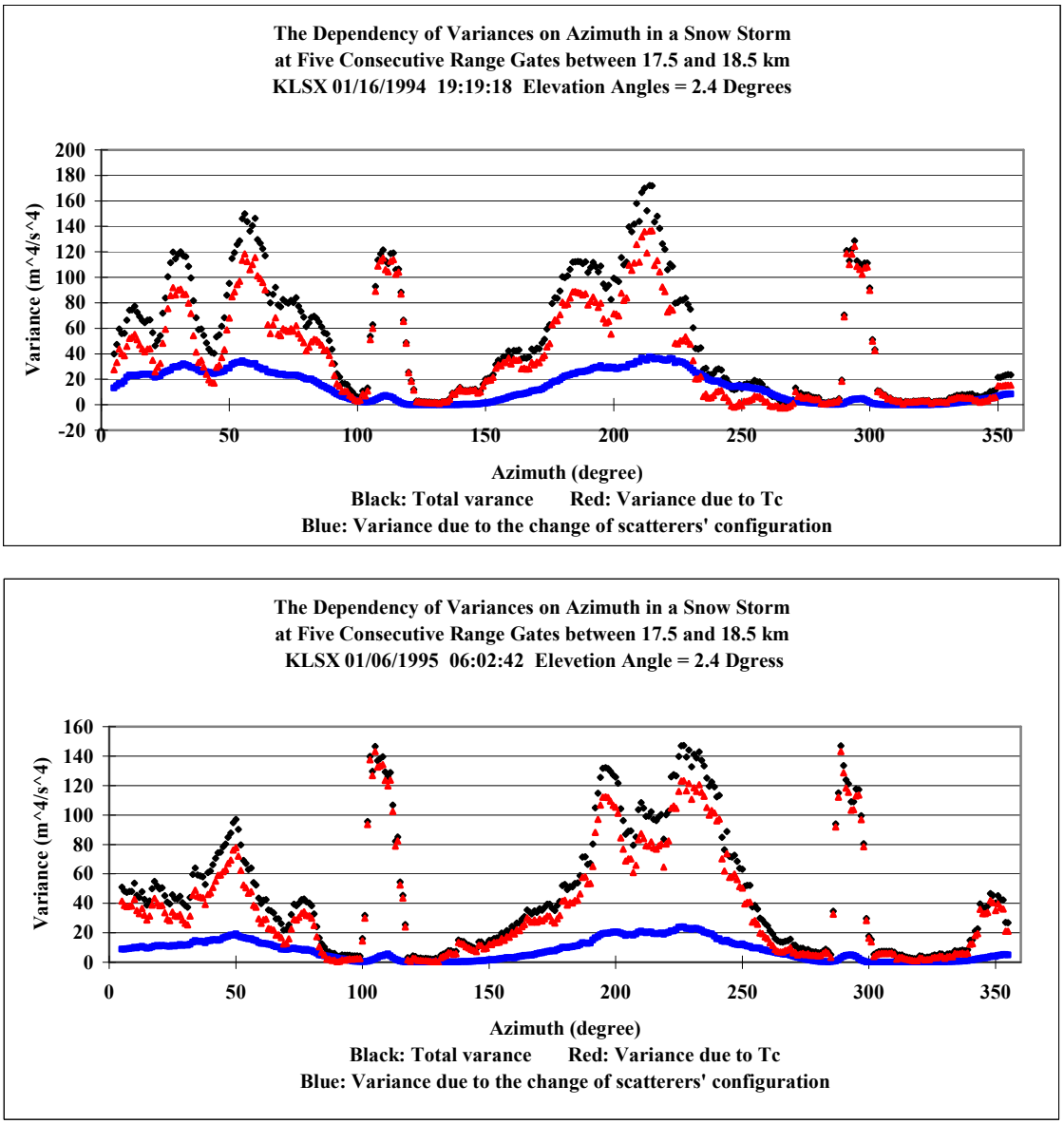

Fig. 4. Azimuth dependence of the three major variances: $\mathrm{Var}_{\mathrm{obs}}\left[\overline{\hat{\sigma}_{\mathrm{v}}^{2}}^{(\mathrm{e})}\right]$ (black), $\mathrm{Var}_{\mathrm{v}}\left[T_{\mathrm{c}}^{(\mathrm{e})}\right]$ (red), $\mathrm{Var}_{\mathrm{sc}}\left[\overline{\hat{\sigma}_{\mathrm{v}}^{2}}^{(\mathrm{e})}\right]$ (blue). Data collected with KLSX as in Fig.1.

values. Asexplained before, the broad peaks of variance centered at about 50° and 230° is related to the influence of shear of the mean radial wind component.

The important point is that most azimuths and for both cases $\mathrm{Var}_{\mathrm{v}}\left[T_{\mathrm{c}}^{(\mathrm{e})}\right]$ is larger than $\mathrm{Var}_{\mathrm{sc}}\left[\overline{\hat{\sigma}_{\mathrm{v}}^{2}}^{(\mathrm{e})}\right]$ (i.e., the variance due to fluctuations of weather signals, the benchmark for

assessing performance for measuring spectrum width estimators). If turbulence measurement is the main purpose for using spectrum width data, $T_c^{(e)}$ is then significant whenever $\mathrm{Var}_v\left[T_c^{(e)}\right]$ is comparable to $\mathrm{Var}_{sc}\left[\overline{\hat{\sigma}_v^2}^{(e)}\right]$

4. Another method to calculate variance of the coupled term

By computing term by term the variances in Eq. (6) as explained in Section 3, $\mathrm{Var}_v\left[T_c^{(e)}\right]$ was calculated as a function of azimuth. In this procedure, there are two assumptions. One is that the large scale turbulence primarily contributing to $T_c^{(e)}$ is horizontally homogeneous and 2D horizontally isotropic; another is that turbulence primarily contributing to $\overline{\hat{\sigma}_t^2}^{(e)}$ is at least 2D horizontally isotropic. These assumptions enabled us to derive an equation to calculate $\mathrm{Var}_v\left[\overline{\hat{\sigma}_t^2}^{(e)}\right]$. This Section offers another simpler method, not requiring these assumptions, to roughly estimate $\mathrm{Var}_v\left[T_c^{(e)}\right]$. But this alternative approach only yields a lower bound for $\mathrm{Var}_v\left[T_c^{(e)}\right]$. Nevertheless it provides us with a chance to compare $\mathrm{Var}_v\left[T_c^{(e)}\right]$ estimates obtained in section 3d with those obtained in this section.

On the left side of (3a) $\overline{\hat{\sigma}_v^2}^{(e)}$ is a radar measured datum, $\overline{\hat{\sigma}_s^2}^{(e)}$ can be calculated from data (Appendix A), and σ_α^2 is known (section 3*a*). Without $T_c^{(e)}$, the right side of (3a) is a squared variable, and therefore should be never negative. Thus, without $T_c^{(e)}$, the left side should be never negative, unless $\overline{\hat{\sigma}_s^2}^{(e)}$ is an overestimate larger than $\overline{\hat{\sigma}_v^2}^{(e)} - \sigma_\alpha^2$. However, Fig. A3 shows the variance associated with the estimation of $\overline{\sigma_s^2}^{(e)}$ is very small, and Fang (2008, Fig. 9.9) shows $\overline{\sigma_s^2(\vec{r})}^{(e)}$ changes slowly and monotonically with time. Thus, if there are negative values of $\overline{\hat{\sigma}_v^2}^{(e)} - \overline{\hat{\sigma}_s^2}^{(e)} - \sigma_\alpha^2$, the negative values should be primarily attributed to $T_c^{(e)}$.

Fig. 5 shows histograms of $\overline{\hat{\sigma}_v^2}^{(e)} - \overline{\hat{\sigma}_s^2}^{(e)} - \sigma_\alpha^2$ for the two snow storms observed with KLSX. It can be seen that there are many negative values. By discarding the values larger than zero and assuming the negative data represents the negative half the distribution of $T_c^{(e)}$, we subjectively fitted the remaining data with a Gaussian function to estimate $\mathrm{Var}_v\left[T_c^{(e)}\right]$ equal to about 5.3 and 1.7 $m^4 s^{-4}$ respectively for cases in Fig. 5a and 5b. $T_c^{(e)}$ is a random variable with zero mean, but the mean of $\overline{\hat{\sigma}_v^2}^{(e)} - \overline{\hat{\sigma}_s^2}^{(e)} - \sigma_\alpha^2$ is usually larger than zero if $\overline{\hat{\sigma}_t^2}^{(e)}$ > 0. Choosing a zero mean for $\overline{\hat{\sigma}_v^2}^{(e)} - \overline{\hat{\sigma}_s^2}^{(e)} - \sigma_\alpha^2$ and only negative values to fit the Gaussian function gives us a conservative or lower bound estimate of $\mathrm{Var}_v\left[T_c^{(e)}\right]$. These $\mathrm{Var}_v\left[T_c^{(e)}\right]$ values can be compared with the average of those shown in Fig. 4 estimated to be a few tens of $m^4 s^{-4}$. Although $\mathrm{Var}_v\left[T_c^{(e)}\right]$ estimated from the histograms is significantly smaller, they are lower bounds and thus consistent with the average obtained from Fig. 4.

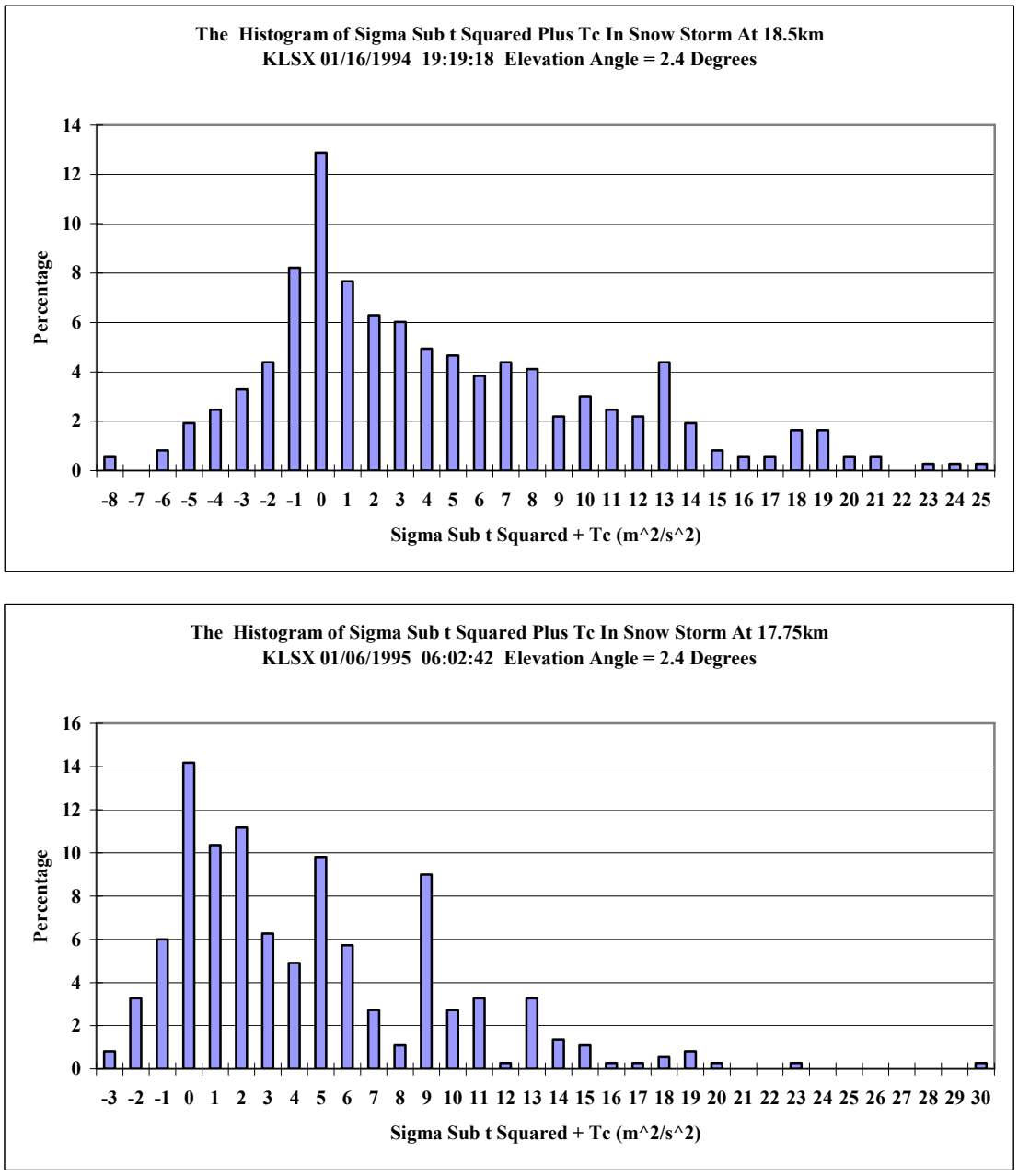

Fig. 5. Histograms of $\overline{\hat{\sigma}_{\mathrm{v}}^{2}}^{(\mathrm{e})} - \overline{\hat{\sigma}_{\mathrm{s}}^{2}}^{(\mathrm{e})} - \sigma_{\alpha}^{2}$ for data collected with KLSX as in previous figures.

5. Summary and conclusions

The second central moment of the estimated Doppler spectrum has been shown not to be a *weighted* sum of second central moments associated with each independent spectral broadening mechanism, as has been commonly accepted, and there is an additional term $T_{\mathrm{c}}^{(\mathrm{e})}$. This term is a weighted cross product of the shears of mean wind and turbulence across the radar's resolution volume $\mathrm{V}_{6}^{(\mathrm{e})}$. This study reported herein, using weather radar data, focuses on estimating the intensity and significance of $T_{\mathrm{c}}^{(\mathrm{e})}$. Examination of data from stratiform weather shows that the coupled term T_c

is significant for weather where vertical shear is strong. It is found that most values of the variance $\mathrm{Var}_{\mathrm{v}}\left[T_{\mathrm{c}}^{(\mathrm{e})}\right]$ of the coupled term are larger than the variance $\mathrm{Var}_{\mathrm{sc}}\left[\overline{\hat{\sigma}_{\mathrm{v}}^{2}}^{(\mathrm{e})}\right]$ due to fluctuations of weather signal (Fig. 4). Thus, the coupled term can impede the accurate measurement of turbulence in strong shear layers. Furthermore, the variance $\mathrm{Var}_{\mathrm{q}}\left[\overline{\hat{\sigma}_{\mathrm{v}}^{2}}^{(e)}\right]$ associated with quantization of the recorded spectrum width data can be larger than 1 m^4 s^{-4} (Section 2*b*), and therefore it needs to considered if turbulence in strong shear layers is to be accurately measured.

Acknowledgement:

This work was supported by NSF Grant ATM0715235 and funding from NOAA/Office of Oceanic and Atmospheric Research under NOAA-University of Oklahoma Cooperative Agreement NA17RJ1227.

APPENDIX A

Assessing the Intensity of the Squared Spectrum Width due to Shear

In order to simplify problem, the calculation of $\overline{\hat{\sigma}_{\mathrm{s}}^{2}}^{(\mathrm{e})}$ and its variance is conducted assuming a uniform vertical shear layer wherein the wind speed and wind direction are

$$V_{\mathrm{h}} = k_{\mathrm{v}} z + b_3, \quad \varphi_{\mathrm{w}} = k_{\varphi} z + b_4. \qquad \text{(A1a, b)}$$

where k_{v}, k_{φ}, b_3 and b_4 are constants that can be determined by least square fitting, to (A1), the V_{h} and φ_{w} data, obtained from a VAD analysis of the radial velocities as a function of azimuth for every $\mathrm{V}_{6}^{(\mathrm{e})}$ on a circle of constant range. Thus one pair of V_{h} and φ_{w} (Fig. A1) is obtained for each circle of radial velocities. To obtain reliable wind profiles with good resolution, the VAD analysis is performed at each range between 5 and 20 km (at 20 km, beam width $\sigma_{\theta} r_0$ is about 100m) whenever there are at least 240 radial velocities available on the constant range circle for each of elevation angles. Therefore an ensemble of V_{h}s and φ_{w} s are obtained.

The pink lines are the least squares linearly fitted profiles of horizontal wind speed and direction; each blue point is the wind speed and direction obtained from a single VAD analysis of radial velocities on a circle at a single range. The V_{h}, φ_{w} data ensemble (Fig. A1) shows a case of a relatively uniform shear layer between 400 and 1100 m; a similar uniform layer of slightly weaker shear was obtained for the snow storm on 6 January 1995 (Fang 2008).

Under the condition the weighting functions and reflectivity are product-separable, Doviak and Zrnić (2006) showed that, if radial velocity is linear across the radar beam, $\overline{\sigma_{\mathrm{s}}^{2}}^{(\mathrm{e})}$ can be separated into three contributions, expressed as:

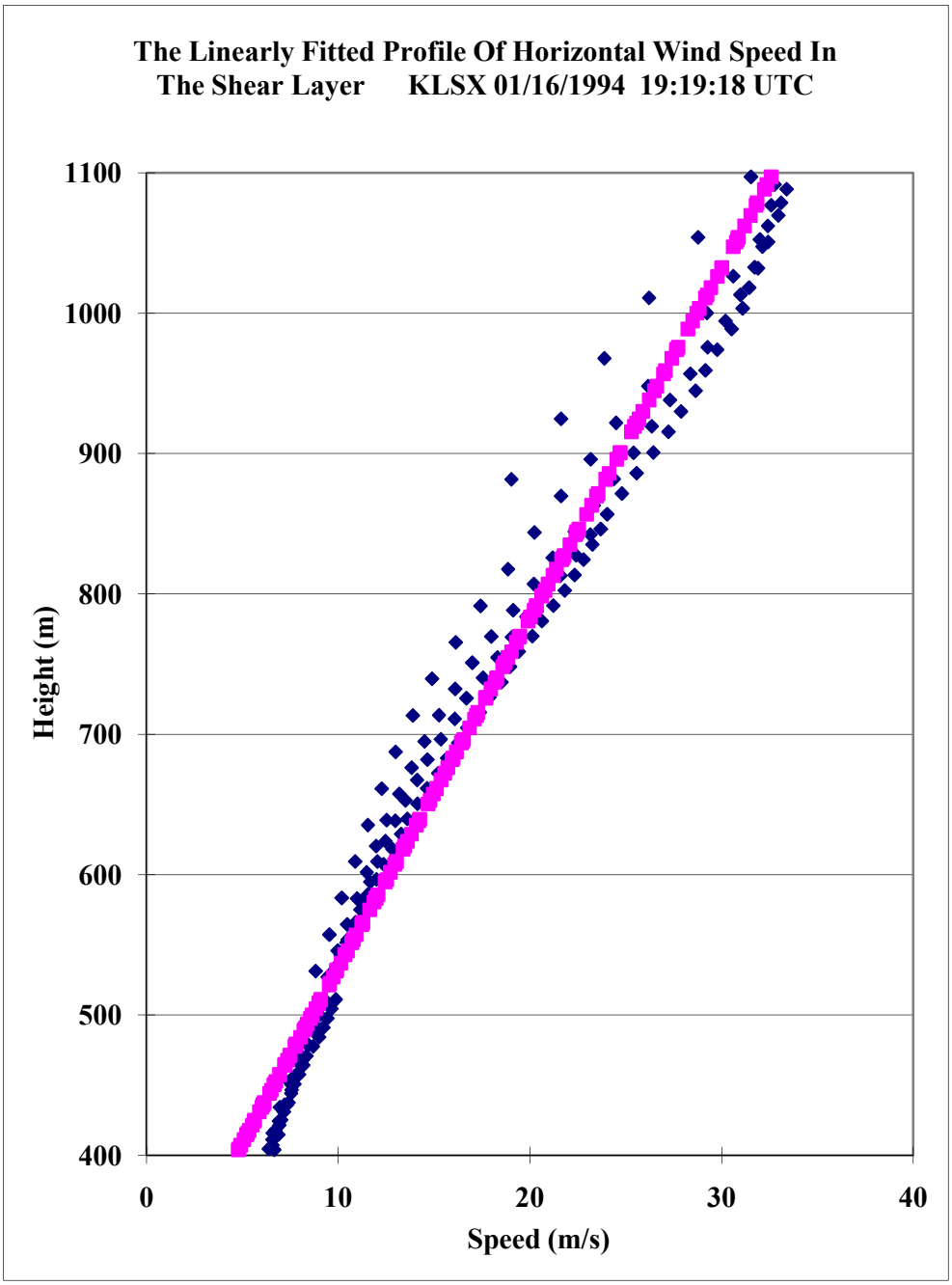

Fig. A1a. VAD derived data (blue points) and the linearly fitted profile (pink) of horizontal wind speed V_h in a snow storm observed by KLSX at 1919 UTC 16 January 1994.

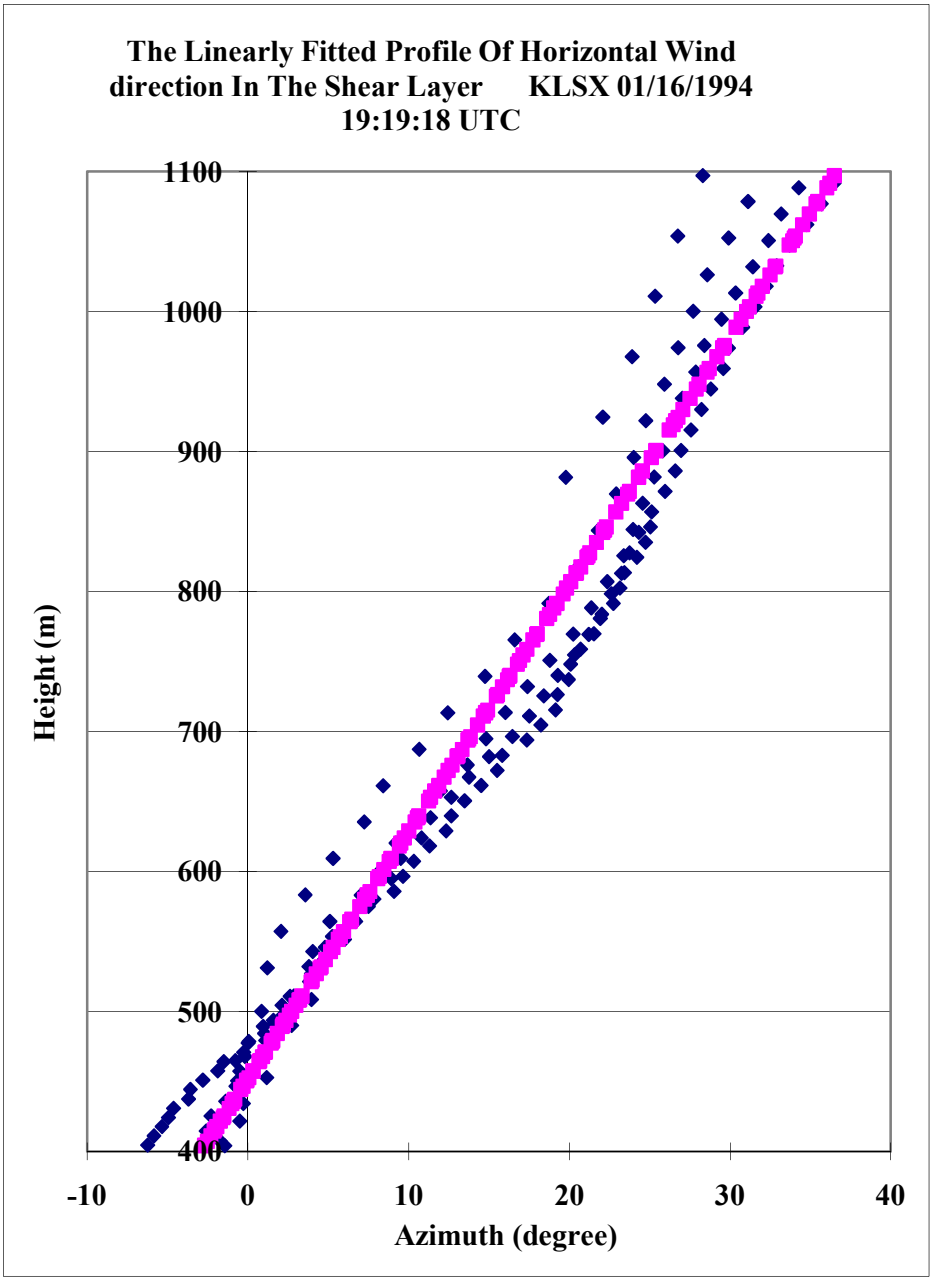

Fig. A1b. Same as Fig. A1a, but for the horizontal wind direction φ_w .

$$\overline{\sigma_s^2}^{(e)} = (k_r\sigma_r)^2 + \left[k_\varphi r_0 \sigma_{\varphi e}(\theta_0)\right]^2 \sin^2\theta_0 + (k_\theta r_0 \sigma_\theta)^2 \quad \text{(A2a)}$$

where θ_0 is the zenith angle, k_r, k_φ and k_θ are shears in radial, azimuth and elevation directions respectively. σ_θ^2 and $\sigma_{\varphi e}^2(\theta_0)$ are second central moments of the two-way antenna power pattern in the elevation and azimuth directions, and σ_r^2 is the second central moment of the weighting function in radial direction. Note that (A2a) differs from that presented by Doviak and Zrnić (2006)

because (A2a) accounts for the change in $\sigma_{\varphi e}(\theta_0)$ with change in zenith angle and also accounts for the change in $\sigma_{\varphi e}(\theta_0)$ for a scanning beam by replacing $\sigma_{\varphi}(\theta_0)$ with the effective azimuth beamwidth $\sigma_{\varphi e}(\theta_0)$. For a circular symmetric (i.e., when not scanning) beam

$$\sigma_\theta^2 = \frac{\theta_1^2}{16\ln 2} \quad , \quad \sigma_{\varphi e}(\theta_0) = \frac{\theta_{1e}^2}{16(\ln 2)\sin^2\theta_0}, \text{ (A2b, c)}$$

where θ_1 is one-way half power beam width. For a rectangular transmitted pulse and a receiver with Gaussian shaped response (Doviak and Zrnić, 2006, Section 5.3),

$$\sigma_r^2 = \left(\frac{0.35c\tau}{2}\right)^2 \quad \text{(A2d)}$$

approximates the range weighting function of the WSR-88D.

Fang (2008, Section 9.3) has shown that k_r, and k_φ are at least one order magnitude smaller than k_θ, so that (A2a) reduces to

$$\overline{\hat{\sigma}_s^{2(e)}} \approx \sigma_{s\theta}^2 = \left(k_\theta r_0 \sigma_\theta\right)^2, \quad \text{(A3)}$$

Because $\theta_0 \approx \pi/2$ (A3) can be then be expressed as,

$$\overline{\hat{\sigma}_s^{2(e)}} \approx \left[k_v \cos(\varphi_0 - \varphi_w) + k_\varphi V_{h0} \sin(\varphi_0 - \varphi_w)\right]^2 \left(r_0 \sigma_\theta\right)^2. \text{ (A4)}$$

$\overline{\hat{\sigma}_s^{2(e)}}$ is plotted in Fig. A2 for the data presented in Fig. A1. Very similar results are obtained for the snow storm case one year later (i.e., 6 January 1995), but $\overline{\hat{\sigma}_s^{2(e)}}$ is weaker.

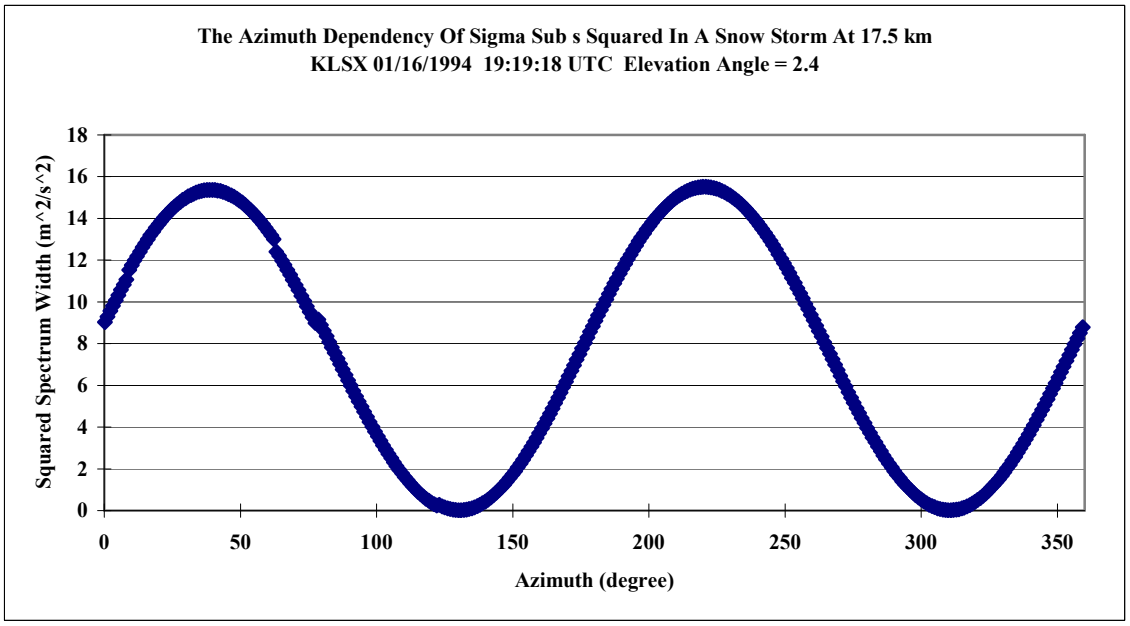

Fig. A2. The spectrum width squared $\overline{\hat{\sigma}_s^{2(e)}}$ due to mean wind shear of the fitted profile in Fig. A1.

Using all the V_h and φ_w data within the shear layer between 400 and 1100 m, the variances of V_h and φ_w are calculated about a linear fit to the data. Thus using (A4) it can be shown (Fang, 2008, Section 9.3) $\mathrm{Var}\left[\overline{\hat{\sigma}_s^{2(e)}}\right]$ is given by

$$Var\left[\overline{\hat{\sigma}_s^2}^{(e)}\right] = \left(r_0\sigma_\theta\right)^2 \left\{ \mathrm{Var}\left[V_h(z)\right] 4k_\varphi^2 \left[k_v \cos(\varphi_0 - \varphi_w) + k_\varphi V_h \sin(\varphi_0 - \varphi_w)\right]^2 \right.$$
$$\times \sin^2(\varphi_0 - \varphi_w) + 4\mathrm{Var}\left[\varphi_w(z)\right]\left[k_v \cos(\varphi_0 - \varphi_w) + k_\varphi V_h \sin(\varphi_0 - \varphi_w)\right]^2$$
$$\left. \times \left[k_v \sin(\varphi_0 - \varphi_w) - k_\varphi V_h \cos(\varphi_0 - \varphi_w)\right] \right\} \quad \text{(A5)}$$

Fig. A3 shows the time series of $\mathrm{Var}\left[\overline{\hat{\sigma}_s^2}^{(e)}\right]$ calculated using (A5) for the snow storm that produced the data shown in Fig. A1. It can be seen $\mathrm{Var}\left[\overline{\hat{\sigma}_s^2}^{(e)}\right]$ is very small (it is even smaller for the snowstorm on 6 January 1995). Thus it is expected that the calculated $\overline{\hat{\sigma}_s^2}^{(e)}$ is very close to the expected value $\overline{\sigma_s^2}^{(e)}$.

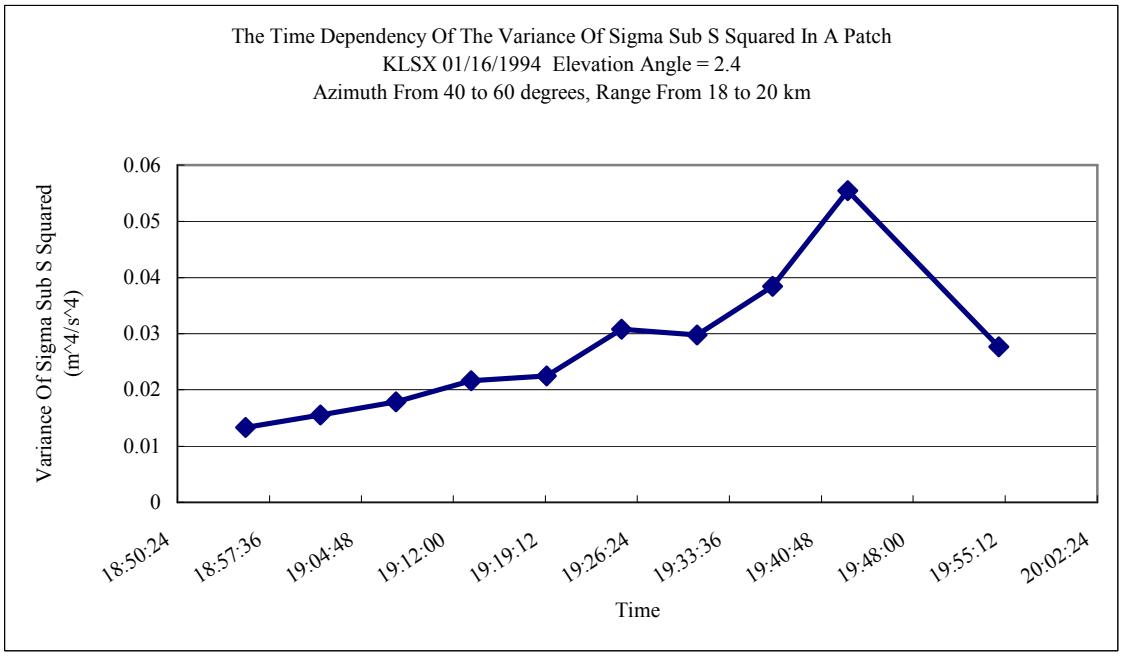

Fig. A3. The time series of $\mathrm{Var}\left[\overline{\hat{\sigma}_s^2}\right]$ for the same snow storm data presented in Fig. A1.

APPENDIX B

Quantization Variance

If a random variable *x* has a uniform probability density function between –*w*/2 and *w*/2, that is p(*x*) = 1/*w*, the variance of *x* then is

$$\mathrm{Var}[x]=\int_{-\frac{w}{2}}^{\frac{w}{2}}\frac{1}{w}x^2dx=\frac{1}{3}\frac{1}{w}\left[\left(\frac{w}{2}\right)^3-\left(-\frac{w}{2}\right)^3\right]=\frac{w^2}{12}. \quad \text{(B1a)}$$

If the distribution of $\overline{\hat{\sigma}_v}$ is uniform across the quantization interval, the quantization variance is given by (Shrader, 1970, p.17-50),

$$\mathrm{Var}_q\left[\sqrt{\overline{\hat{\sigma}_v^2}^{(e)}}\right]=\frac{(\Delta\sigma_v)^2}{12}, \quad \text{(B1b)}$$

where $\Delta\sigma_v$ is the quantization interval; for the WSR-88D $\Delta\sigma_v$ = 0.5 m s^{-1}, and therefore

$$\mathrm{Var}_q\left[\sqrt{\overline{\hat{\sigma}_v^2}^{(e)}}\right]=\frac{0.5^2}{12}=0.02 \text{ m}^2\text{s}^{-2}. \quad \text{(B1c)}$$

What we need in the variance equation (5) however is $\mathrm{Var}_q\left[\overline{\hat{\sigma}_v^2}^{(e)}\right]$ not $\mathrm{Var}_q\left[\sqrt{\overline{\hat{\sigma}_v^2}^{(e)}}\right]$. Applying the methods outlined by Papoulis and Pillai (Papoulis and Pillai, 2003, p.150), it can be shown that

$$\mathrm{Var}_q\left[\overline{\hat{\sigma}_v^2}^{(e)}\right]=4\mathrm{E}_v^2\left[\sqrt{\overline{\hat{\sigma}_v^2}^{(e)}}\right]\mathrm{Var}_q\left[\sqrt{\overline{\hat{\sigma}_v^2}^{(e)}}\right], \quad \text{(B2)}$$

which is valid for distributions of $\sqrt{\overline{\hat{\sigma}_v^2}^{(e)}}$ that are sufficiently narrow so that a linear approximation (i.e. to the squared dependence of $\overline{\hat{\sigma}_v^2}^{(e)}$ on $\sqrt{\overline{\hat{\sigma}_v^2}^{(e)}}$) about the expected value is maintained for most of the data contained in the distribution. The expectation $\mathrm{E}_v\left[\sqrt{\overline{\hat{\sigma}_v^2}^{(e)}}\right]$ is approximated using a running spatial average of spectrum width data from 10 radials at 5 consecutive range locations. Then quantization variance $\mathrm{Var}_q\left[\overline{\hat{\sigma}_v^2}^{(e)}\right]$ is calculated using (B2) and (B1c).

Fig. B1 shows the azimuth dependence of $\mathrm{Var}_q\left[\overline{\hat{\sigma}_v^2}^{(e)}\right]$ vs azimuth angle.

Another issue associated with $\mathrm{Var}_q\left[\overline{\hat{\sigma}_v^2}^{(e)}\right]$ is whether it should be added to or subtracted from $\mathrm{Var}_{obs}\left[\overline{\hat{\sigma}_v^2}^{(e)}\right]$. In order to determine this, let's consider a random variable *x* uniformly distribute between -1.5 and 1.5 with a zero mean. From Eq. (B1a), the variance, in absence of quantization, is $Var[x]=\frac{3^2}{12}=0.75$. Now consider x is quantized with an interval 1. That is, if *x* lies between -1.5 and -0.5, it takes the value -1; if *x* lies between -0.5 and 0.5, it takes the value 0; if *x* lies between 0.5 and 1.5, it takes the value 1; The variance for the quantized *x* is then

$$Var[x]=\frac{1}{3}\left[(x_1-\bar{x})^2+(x_2-\bar{x})^2+(x_3-\bar{x})^2\right]=\frac{1}{3}\left[(-1)^2+(0)^2+(1)^2\right]=0.667.$$

Thus, quantization decreases the variance of the observed variable and quantization variance should therefore be added to the left hand side of (5) which becomes,

$$\mathrm{Var}_{obs}\left[\overline{\hat{\sigma}_v^2}^{(e)}\right]+\mathrm{Var}_q\left[\overline{\hat{\sigma}_v^2}^{(e)}\right]=\mathrm{Var}_v\left[\overline{\hat{\sigma}_t^2}^{(e)}\right]+\mathrm{Var}_v\left[T_c^{(e)}\right]+\mathrm{Var}_{sc}\left[\overline{\hat{\sigma}_v^2}^{(e)}\right] \quad \text{(B3)}$$

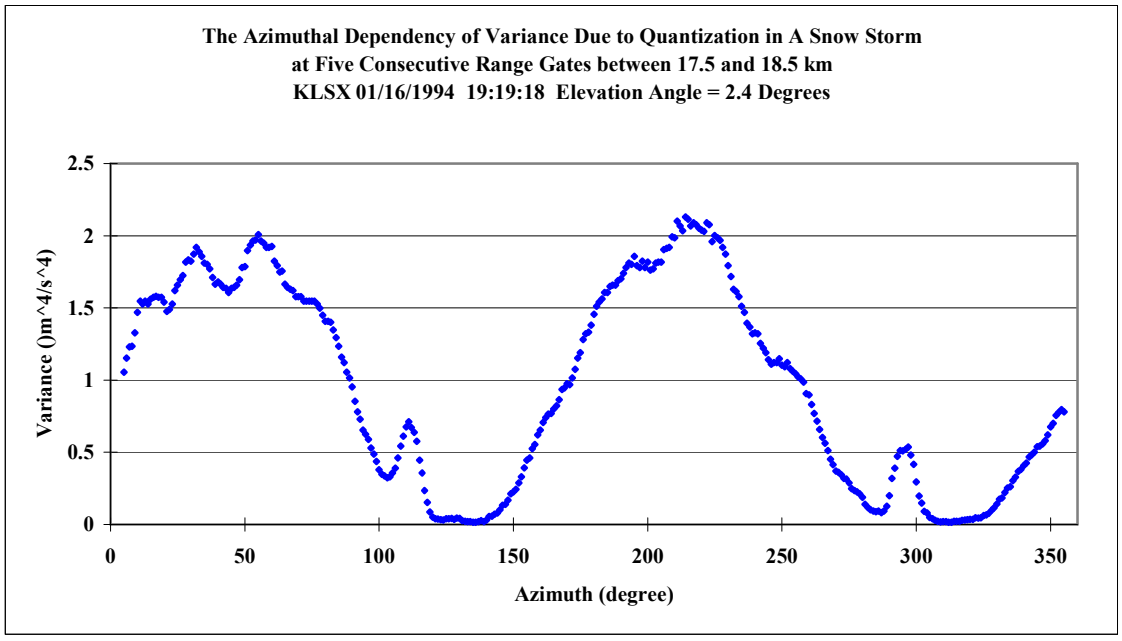

Fig. B1 Azimuth dependence of quantization variance $\mathrm{Var}_q\left[\overline{\hat{\sigma}_v^2}^{(e)}\right]$ for a snow storm observed by KLSX data presented in Fig. 1a.

REFERENCES

Batchelor, G. K., 1960: The theory of Homogeneous Turbulence, reprinted by Jarrold & Sons, LTD., Norwich, 195pp.

Doviak, M. Fang, V. Melnikov, and G. Zhang, 2008: Theoretical and practical considerations in using spectrum width data. *ERAD 2008-The Fifth European Conference on Radar in Meteorology and Hydrology*, Finish Meteorological Institute, 4 pp.

Doviak, R. J. and D. S. Zrnić, 2006: *Doppler radar and weather observations*. 2nd ed. Dover Publications, 562 pp.

Endlich, R. M., R. C. Singleton, and J. W. Kaufman, 1969: Spectral Analysis of Detailed Vertical Wind Speed Profiles. *J. Atmos. Sci.*, **26**, 1030-1041.

Fang M, Doviak R. J. 2008: Coupled Contributions in the Doppler Radar Spectrum Width Equation. Journal of Atmospheric and Oceanic Technology: In Press.

Fang, M., 2008: The spectrum width equations for Doppler weather radar and the coupling of spectral broadening terms. A *Dissertation*, University of Oklahoma, 178 pp.

Hocking, W. K., 1988: Two years of continuous measurement of turbulence parameters in the upper mesosphere and lower thermosphere made with a 2-MHz radar. *J. Geophys. Res.*, **93**, 2475-2491.

Nastrom, G., and K. Gage, 1985: A Climatology of Atmospheric Wavenumber Spectra of Wind and Temperature Observed by Commercial Aircraft. *J. Atmos. Sci.*, **42**, 950–960.

Papoulis, A. and S. U. Pillai, 2004: *Probability, Random Variables, and Stochastic Processes*, McGraw Hill Book Co., 852 pp.

Shrader, W. M., 1970: MTI Radar, *Radar Handbook*, McGraw Hill Book Co., New York, NY.

Vinnichenko, N. K., and J. A. Dutton, 1969: Empirical studies of atmospheric structure and spectra in the fee atmosphere, *Radio Sci.* **4**, 1115-1126.

Zrnić, D. S., and R. J. Doviak, 1989: Effect of Drop Oscillations on Spectral Moments and Differential Reflectivity Measurements. *J. Atmos. Oceanic Technol.*, **6**, 532–536.